1 × 3 beam splitters based on multimode interference effect in Photonic Crystal waveguides formed by holographic lithography

1×3 beam splitters based on multimode interference effect in Photonic Crystal waveguides formed by holographic lithography

X X Shen[1] and Y Z Ren

Shen Zhen Institute of Information and technology, ShenZhen, 518072, China

[1] E-mail: shenxx@sziit.edu.cn

Abstract.A study on compact 1×3beam splitter based on multimode interference effect in Photonic crystal waveguides formed by holographic lithography was presented. The 1×3 beam splitter was designed and characterized using PWE calculation and FDTD simulations. Simulation results show that this kind of beam splitters can be compact and easily fabricated. For TE mode, the input field can be divided into three parts equally and obtain a high total transmission simultaneously by modulation of the effective index of coupling PhC rows, while with a fixed length of MMI region.

1. Introduction

The usages of large scale photonic Integrated Circuits (PICs)in optical systems can help to improve their reliabilities and simplify the design.Since Photonic Crystals (PhCs) have the capability of controlling light waves in an ultra-small area and can also be easily fabricated, using PhCs has become a promising technology in large-scale photonic integrated circuits. Optical components with PhC-based waveguide have also been investigated extensively. The light waves propagated by evanescent coupling between the neighboring cavities in coupled cavities which were called as coupled resonators [1-2] or by nanojet coupling and Bragg reflection in the light defects named as photonic crystal waveguides (PhCWs) [3-6]. Multiway beam splitters are one of the central building blocks among the integrated components in PICs especially in wavelength division multiplexing systems; however, most of the work has focused on the performance of single-mode PhCW for 1×2 optical beam splitter. Recently, multimode interference (MMI) effects have been applied in many fields in integrated optics, such as wavelength de-multiplexer based on self-imaging phenomena in PhCWs [7], terahertz switches in silicon triangular PhCW [8], and TE and TM polarization splitters [9]. Multiway beam splitter based on MMI effect of PhC waveguides had also been investigated Recently [10-12], the most significant advantage for these components based on every-other line-defect PhCWs is the ultra-compact design, since the beat-length in the MMI region is much smaller than in MMI region of conventional photonic waveguides, and moreover, the adjacent outputwaveguides have to be separated far enough to minimize coupling between them for conventional waveguides, yet a rather wide multi-mode section is required.

For the fabrication of photonic crystal waveguides, holographic lithography (HL) has its unique advantages such as one-step recording and the ability of obtaining inverse lattice by using a template compared with many other methods, thus to extend the study of propagation properties to 2D HL structures is very useful and important. In this work, we introduced a compact multiway beam splitter

based on MMI effects between 2D honeycomb PhC waveguides formed by single-exposure holographic interference fabrication methods. As thin air-slab PhCW devices with high transmittance can be easily fabricated and integrated with other PIC building blocks, we investigated the 1×3 beam splitter based on a dielectric slab with the dielectric constant n=3.4 for silicon. And the plane wave method (PWM) with wave number of 729 is employedto assure the convergence of numerical calculations for dispersion diagrams, then the propagating properties of beam splitter are demonstrated by finite-differencetime-domain (FDTD) simulations with perfectly matched layer (PML) boundary conditions [13]. Due to the desired conditions for the case under study, only the TE modes areconsidered here (the M field is vertical to the slab plane).

2. MMI effect principle and theoretical analysis

Multi mode interference in defect waveguides leads to the self-imaging effect, which is a property of multimode waveguides, means an input field profile is reproduced for single or multiple images at periodic intervals along the propagation axis. And this effect strongly depends on the number of modes, propagation constants, and modal field patterns [14].

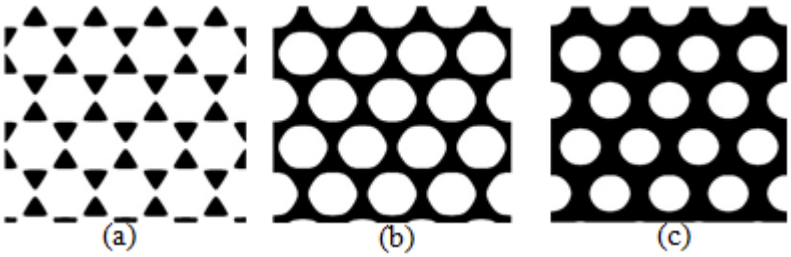

Figure 1. Variation of the shape and size of the cross section of air columns with different I_t and filling ratio FR. (a)I_t=1.95, FR=21.23 %; (b) I_t =2.3, FR=42.03%; (c) I_t =2.9, FR=58.96%.

The multiway beam splitter is based on 2D honeycomb photonic crystals formed by holographic lithography (HL PhC): 3 mutually coherent laser beams are made to interfere, producing 2D patterns of light and dark areas repeated on a scale proportional to the wavelength of the beams used, then use proper dielectric materials to record these interference patterns, 2D crystalline structures can be formed. The 2D holographic structure considered in this paper is determined by the intensity distribution of interference field [15]

$$I = 3 + \cos\left[\frac{2\pi}{\sqrt{3}a}(2y)\right] + \cos\left[\frac{2\pi}{\sqrt{3}a}(\frac{-3}{\sqrt{3}}x + y)\right] + \cos\left[\frac{2\pi}{\sqrt{3}a}(\frac{-3}{\sqrt{3}}x - y)\right] \quad (1)$$

Here, a is the lattice constant. The total exposure is $I\delta$t, where δt is exposure time. For a certain recording material there is a special value of total exposure above or below which the corresponding region of the recording material will be photopolymerized. For brevity here we use just the light intensity expression as shown in Eq. (1) and denote the light intensity threshold corresponding to the exposure threshold as I_t,(I_t ε(1.5, 6) for Eq. (1)). And the first constant in Eq. (1) has no essential effect since we can change the light threshold I_t to compensate it. The region with light intensity below$I_t$can be developed and the region above it will remain due to photo polymerization for negative photoresist, we may wash away the region of $I < I_t$ to get a normal structure. By filling this structure with a material of high dielectric constant and then removing the template with a proper developer, or using positive photoresist in exposure an inverse structure can be obtained. In our situation, we used the inverse structure which means that the dielectric constant distribution ε(x, y) of result lattice should be 1 in the region I(x, y)>I_t, represented by the white part (air); and 11.56 in the region I(x,y)<I_t, represented by black part (Si with refractive index n=3.4). Several lattices which shown in Figure 1 for investigation, here (a), (b) and (c) are the shape and size of the cross section of air columns with different I_t and filling ratio FR. We calculated the photonic band diagrams for the relative honeycomb

holographic lattices with varied I_t, in order to analyze defect modes in PhCWs, the dependence of the photonic bandgap (PBG) on I_t was shown in Figure 2, extracted from band structure calculations when I_t changes from 1.9 to 3.3. The dashed area represented the distribution of PBG for TE mode using normalized frequency units ($\omega a/2\pi c$), and the red dotted line indicate the corresponding relative band gap (measured by gap to mid-gap ratio $\Delta\omega/\omega_0$).

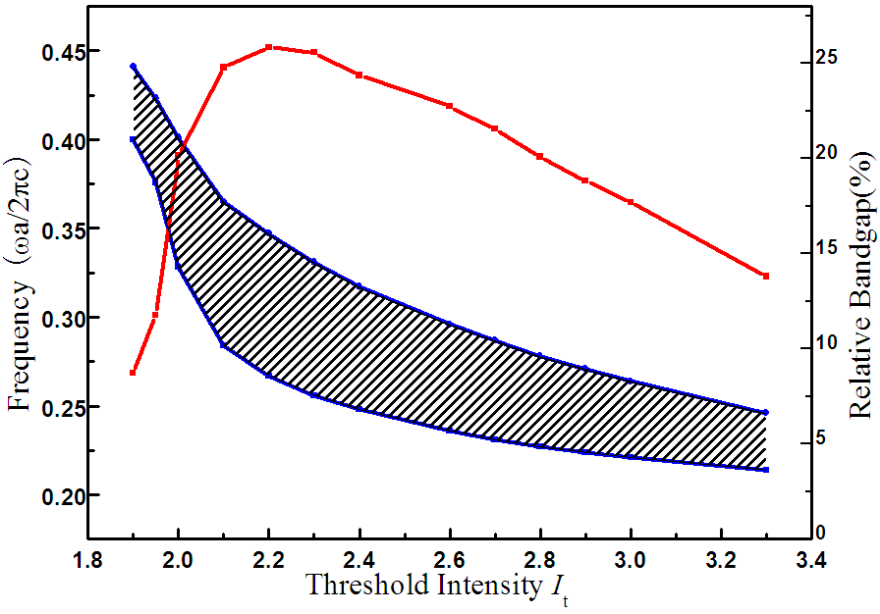

Figure 2. Evolution of photonic band maps for TE polarizations of inverse HL.

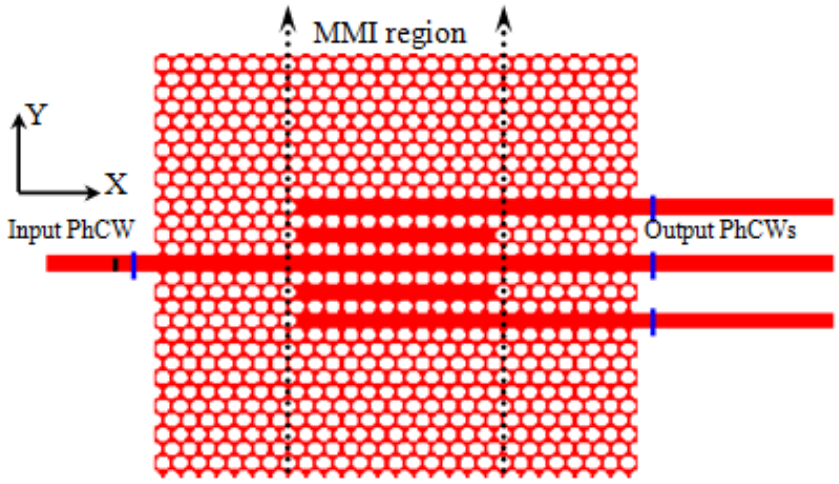

Figure 3. Schematic diagram of beam splitter consist of MMI region and input, output PhCWs.

Tocreate the proposed MMI effect-based beam splitter, the large-area PhC can be patterned in photopolymer by holographic interference in one-step recording at first, and then the defects are introduced by two-photon absorption. Since the two-photo absorption probability depends quadratically on intensity, the polymerization of material is localized only in a small vicinity of order λ^3 (where λ is the laser wavelength) near the focus point, thus the form of defects can be exactly controlled. Consequently using this hybrid method has an advantage in terms of fabrication time and cost for the patterning of large-scale photonic crystal-based integrated systems.In this work, there parts

should include as in Figure 3: a single mode input PhCW, N single-mode output PhCWs and a MMI region with a length of L_M.A waveguidewith the width same to $a$can be obtained as the input regionby removingexactly one single row of air-holes in ΓK direction of the lattice. For MMI region, PhCWs are set along the ΓK direction by removing several entire rows of air-holes and the adjacent PhCWs are separated by one row. Namely, thereare M-1 rows of air-holes between M PhCWs, where M is an integer, and we consider the case with M=5 in this work, the length L_M needs to be optimized and corresponds to the length of n lattices (n must be aninteger to preserve the crystal structure).And for output PhCWs, since the beating length of the adjacent output waveguide is large enough, in our situation the lengths of output PhCWs are short and separated by three rows of air-holes, thus the interaction between output PhCWs is negligible here, which guarantees that the mutliway PhC MMI region-based splitter can be short, while the conventional dielectric MMI coupler had to be set wide and long to minimize coupling of the adjacent output ports [10].

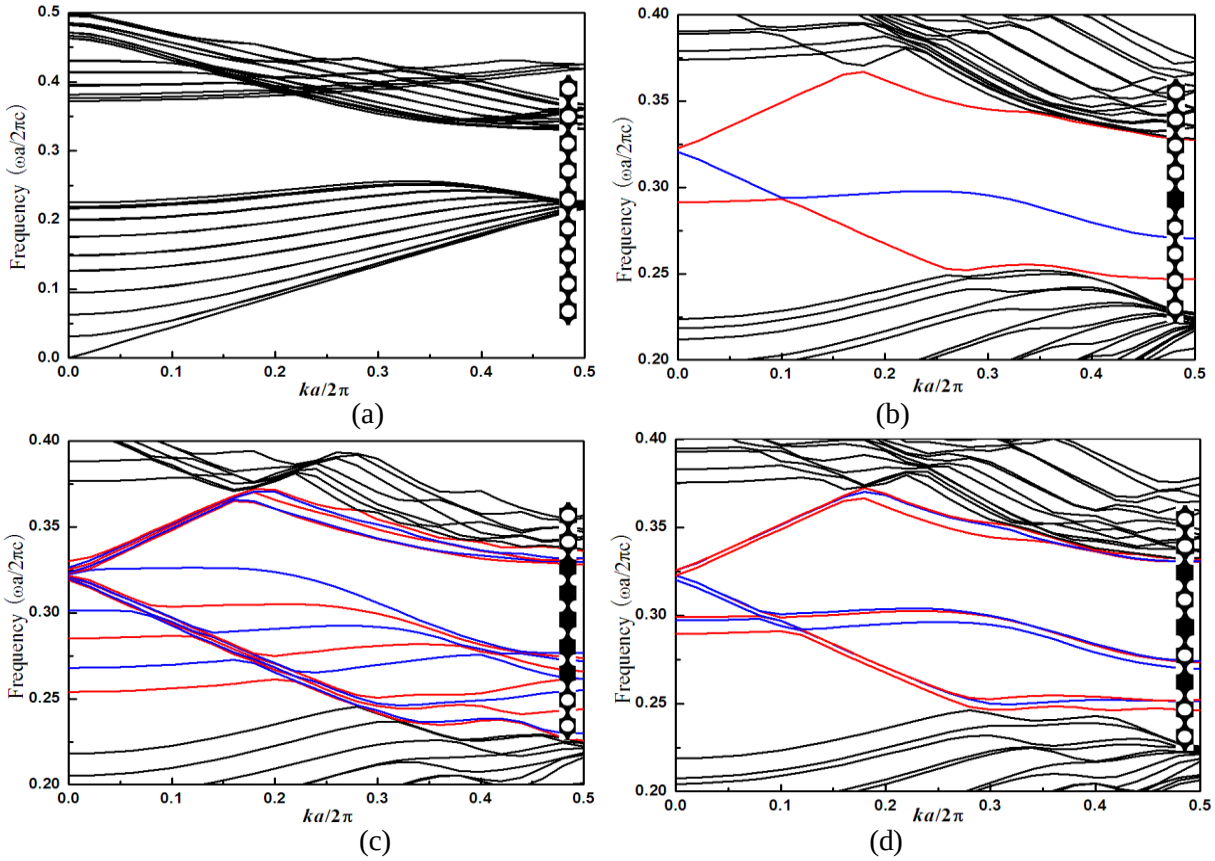

Figure 4. Dispersion diagrams for TE polarization of the PhC and PhCWs using PWE method. The supercells for calculation were shown as the insets. Here PhC modes are represented by black lines, even (odd) defect modes are red (blue) lines. (a)PhC without defects; (b) Input waveguide; (c) MMI region; (d) Output waveguides.

The normalized dispersion diagrams for HL PhC without defect and with threshold intensity I_t=2.3 were given in Figure 4 (a), structure of PhC lattice shown in Figure 1 (b). And Figure 4 (b), (c) and (d) present the dispersion curves for Single- and multi-mode PhCWs. Super-cells for calculation are depicted as inserts. PhC modes are represented by black lines, even (odd) defect modes are red (blue) lines for all these diagrams. Heaton et al had demonstrated that multi way beam splitters based on multimode planar waveguides in the case of symmetric interference [16], the modal field patterns have their own symmetry, even or odd, with respect to the propagation axis, and to excite a superposition of

modes at the excitation frequency is possible. Yet they can be selectively excited either depending on the input position. Since the input field is launched into the MMI region with a symmetric position of y=0, only the even modes represented by red lines can be excited. Compared with Figure 4(a), there exist three defect modes including two even mode in single-mode input PhCW in Figure 4(b); and multi-mode PhCWs support eight and five even modes (Figure 4(c) and Figure 4(d)) in MMI region and output region. Both the bottom and the top of the single-mode frequency span are very close to that of the multi-mode counterpart, only one mode in input PhCW split into five and three modes in MMI region and output PhCWs respectively. From Figure 4 (b), (c) and (d) we can see that the even PBG mode is seen to be flat from k_x=0.4 to 0.5, the variation approaches almost zero in this range, which can be addressed as the slow-light regime. This means that a 1x3 beam splitter is conceivable in this slab design in order to obtaining high transmittance [17].

3. Design and FDTD simulation

The output transmission for this multiway beam splitter depends on the coupling coefficient of MMI region, which was decided by two key parameters: coupling length L_M and shape of PhC lattices. The shape and size of lattice varies with the value of I_t in our situation for HL structure. Since the HL PhC has the biggest relative bandgap when I_t =2.3 shown in Figure 2, we chose this structure for the beam splitter in following discussion. As we know to get high transmission, the three output PhCWs should be placed at the positions of first 3- fold images in our design, which means the length of MMI region L_M should equal to the distance where 3-fold images reproduced, according to self-imaging principle [7], the input field reproduces its direct replica at the position L_d of the MMI region, when L_d satisfy Eq. (2).

$$\beta_n L_d = 2k\pi, k = 1,2,3..... \tag{2}$$

Here β_n is the propagation constant and the subscript n denotes the order of the mode (n=0,2,4….for even modes).The N-fold images should be reproduced at L_N, when

$$L_N = pL_d / N, p = 1,2,3..... \tag{3}$$

With p and N have no common divisor. Eq. (2) produce a set of simultaneous equations, and the equation sets should be simultaneously solved in order to determine the positions of the reproduced images. For the detailed procedure of applying Eq. (2) and (3) to our case, the values of propagation constants at the operating frequency of f=0.33(ωa/2πc) are taken out from the dispersion curves in Figure 4(c) and then lugged into Eq. (2). In general, there are no exact solutions to Eq. (2) due to the periodic nature of sinusoidal functions, but it is possible to determine the nearest positive integer sets, that are simultaneously fit into thee quation sets with acceptable errors. From calculation, the first direct image reproduced at the position of 32a, and the 3-fold image happened at 11a. Thus the total length of the beam splitter can be less than 20a, and if we choose a=0.4μm, the size of this device would be only several microns, which is much more compact compared with the conventional MMI coupler which always has a length of 40~100μm [18].

According to above analyses, the configuration of the HL PhC MMI based multiway beam splitter was given in Figure 3, and is used in 3D FDTD simulations with the grid spacing of a/20.The normalized transmittance is obtained by the transmittance through the theoretical sensors in the right ridge waveguides divided by that through the inputsensor in the left waveguide (denote as blue short line in Figure 3). The normalized transmission for upper and lower output waveguides is about 17.1% and 58.9% for middle output PhCW in FDTD simulation. The beam splitter has not split the input power on average as always expected, thus we change the input frequency in simulation for the same configuration, and found that the three output PhCWs had the average transmission of 21.3% when the input normalized frequency is 0.26. And the H_z field distributions of f=0.26 through the same 1x3 splitter at different simulated time steps are depicted in Figure 5. The blue and red spots correspond to the negative and positive values of the amplitude respectively as indicated in the Figure. Figure 5 (a),

(b) and (c) show the input pulse travels through the beam splitter with time increasing from 20000δt, 50000δt to 70000δt(δt is the finite time step used in simulation, with δt=0.05a/c).

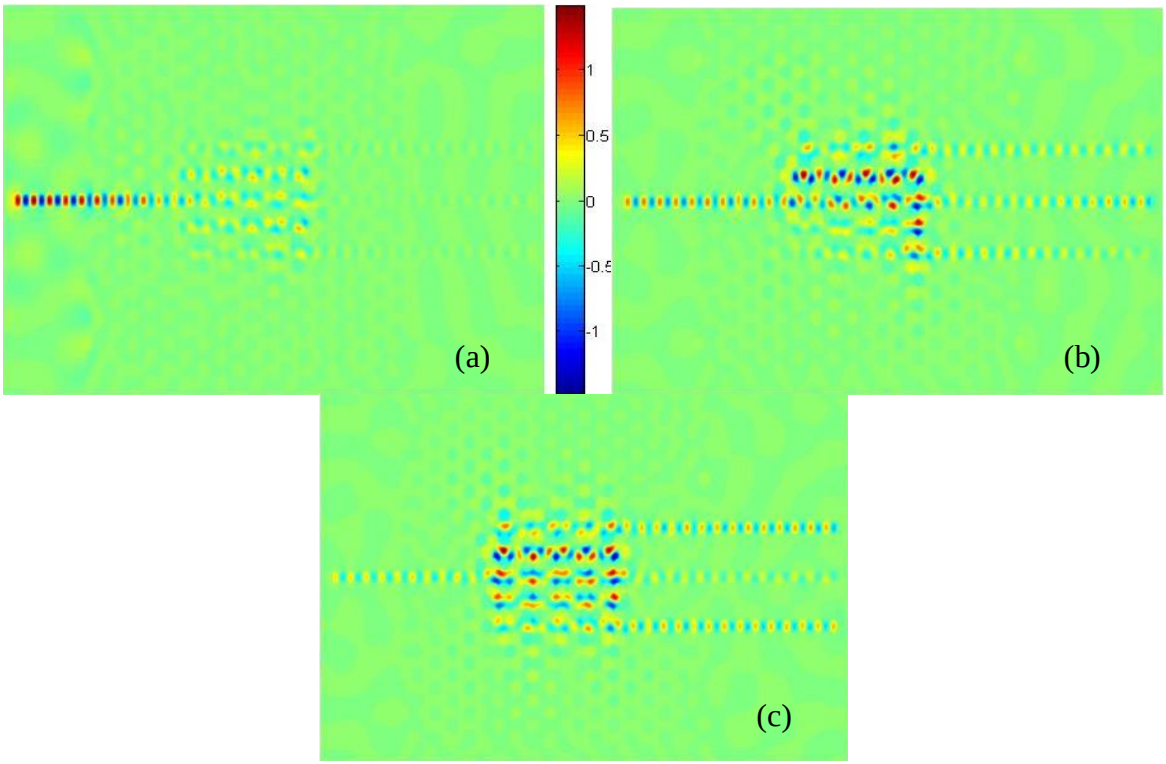

Figure 5. The transverse profile of the magnetic field H_z for f=0.26 at different FDTD time steps: (a) 20000δt; (b) 50000δt; (c) 70000δt.

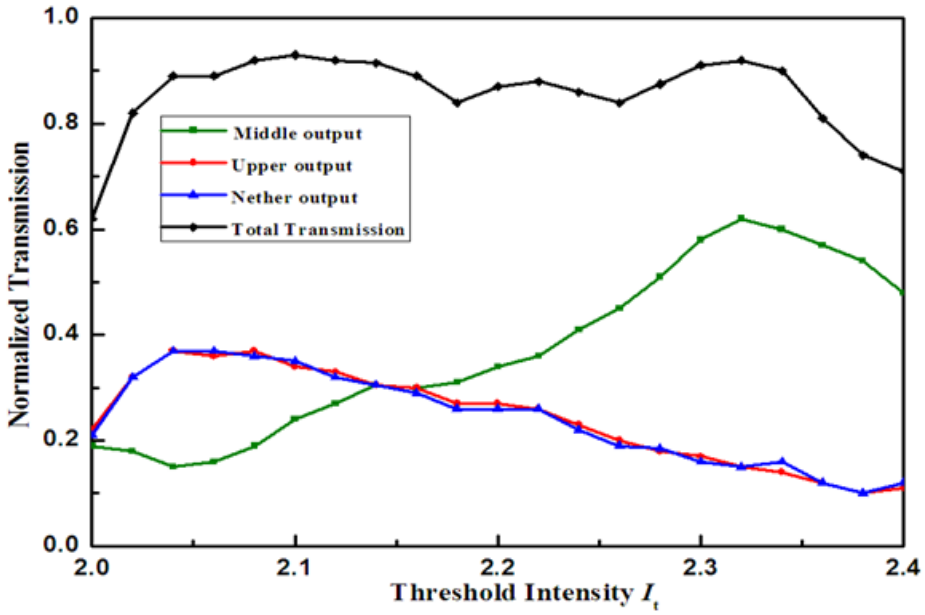

Figure 6. Simulated normalized TE polarized transmittance of all output port with the threshold intensity for modulated HL region varied from 2.0 to 2.4.

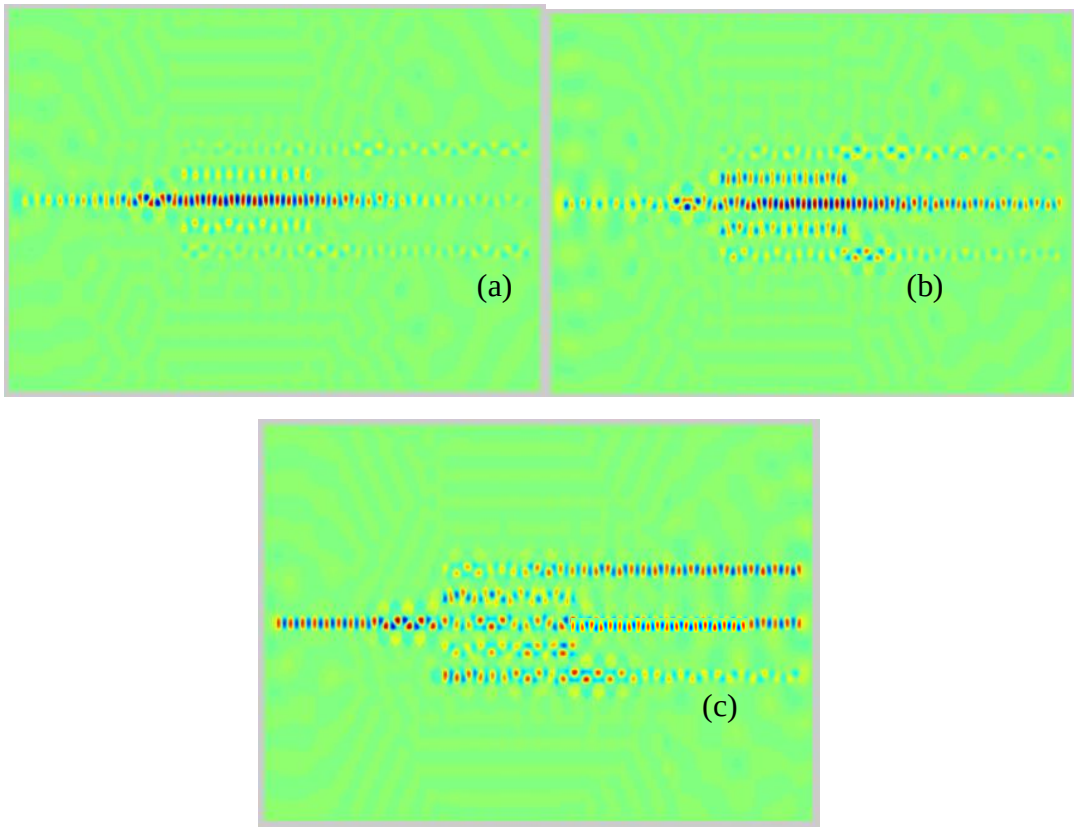

Figure 7. When I_t for modulated region is 2.13, the snapshot of H_z for f=0.33 at different time steps: (a) 20000δt; (b) 50000δt; (c) 70000δt.

Though the FDTD simulations demonstrate that the 1×3 beam splitter can split the input field into three parts equally, the total transmission is only 63.9%. In order to achieve high total transmission and average transmittance on every output port simultaneously, we try to modulate the effective index of the designated PhC regions to change the distribution of the field at the output ports with a fixed coupling length. The output optical power distribution is the superposition of all the excited guided modes, and the field distributions of each single mode can be modulated by changing the effective index of PhC structures between the coupling PhCWs in MMI region, thus we could change the threshold intensity of PhC structures between the upper two PhCWs and the row between the nether two PhCWs from Figure 3, the shape and size of air holes would change consequently, and the effective index either, which could realized in practice using a second exposure. From Figure 2 the evolution of photonic band maps for TE polarizations of inverse HL PhC structures can see that the photonic band gap exist over a wide range of threshold intensity. Since the frequency f=0.33(ωa/2πc) indicated by the black line, lies in the bandgap when I_t changes from 2.0 to 2.4, we use this frequency for calculation, the normalized transmission of each output port as the function of the threshold intensity varies from 2.0 to 2.4 was given in Figure 6. The input power can be divided equally at I_t=2.13, and the responding transmission for each output port is about 30.5%, the total transmission reaches 91.5%. The simulated field distribution for input frequency f=0.33 is shown in Figure 7 when the I_t for modulated PhC region is 2.13. Figure 7 (a), (b) and (c) are the snapshot of H_z when simulated time at 20000δt, 50000δt and 70000δt respectively. Compared Figure 5 with Figure 7, the H_z field patterns agree well with the analyzed results.The average splitting is very sensitive to the operational frequency, and we should change the design for different input frequency, but from Figure 6 the input field can be split almost symmetrically with different splitting proportions at other modulated values.

Furthermore, if the modified regions are not symmetric, the input beam can even be split into multiple output ports with an arbitrary ratio.

4. Conclusions

We presented a 1×3 optical beam splitter based on multimode interference effect in Photonic Crystal waveguides formed by holographic lithography. The beam splitter based on silicon slab with air holes has excellent performance for TE polarization. It could split the input field equally into three output ports by tuning the threshold intensity of the designated PhC structures to modulate the transverse field distribution. The analysis and simulations show that the input beam is dividedafter the MMI region with a length of 11*a* into three output channels, the total output transmission efficiency almost as high as 91.5%. Also this HL PhC based beam splitter can be much more compact in size compared with the conventional MMI coupler even despite the channel number. And considering that HL has its unique advantages such as one-step recording, large scale and low cost in fabrication, holographic structures may have a promising potential when fabricating PhC beam splitters in practice. A more comprehensive study in this field will be our next task.

Acknowledgements

This work is supported by the National Natural Science Foundation (61240015, 51102148), and Shenzhen science and technology plan project (JCYJ20120615101957810, JCYJ20120821162230170), Shenzhen Institute of Information and Technology project (10800-18-010203-0215).

References

[1] I Park, H S Lee and H Lee 2004 *Opt. Express* **12**(15) 3599-3604
[2] T B Yu, M H Wang and J Y Yang 2007 *J. Opt. A, Pure Appl. Opt*. **9**(1) 37-42
[3] Y Zhang, Z J Li and B J Li 2006 *Opt. Express* **14** 2679-2689
[4] A Têtu, M Kristensenand O Sigmund 2005 *Opt. Express* **13**(21) 8606-11
[5] P I Borel, L H Frandsen and O Sigmund 2005 *Electron. Lett* **41**(2) 69-71
[6] M Zhang, R Malureanu, A C Krüger and M Kristensen 2010 *Opt. Express* **18** 14944-49
[7] H J Kim, I Parkand S G Lee 2004 *Opt. Express* **12**(23) 5625-33
[8] Z J Li, Y Zhang and B J Li 2006 *Opt. Express* **14**(9) 3887-92
[9] H B Chen, Y Xu, J L He and Z Hong 2009 *Opt. Commun* **282**(17) 3626-29
[10] T B Yu, H F Zhou, Z Gong, J Y Yang, X Q Jiang and M H Wang 2008 *J. Phys. D Appl. Phys* **41**(9) 095101
[11] M K Moghaddama, M MMirsalehib and A RAttarib 2014 *Photonics and Nanostructures - Fundamentals and Applications* **12**(1) 75-82
[12] W H Yu, P J Yao and P Wang 2013 *International Journal for Light and Electron Optics* **124**(22) 5489-91
[13] X Y Ao and S L He 2004 *Opt. Lett* **29**(21) 2542-44
[14] L B Soldano and E C M Pennings 1995 *J. LightwaveTechnol* **13**615-627
[15] X X Shen, Y Z Ren and Z W Zhou 2013 *Superlattices and Microstructures* **64** 303-310
[16] J M Heaton, R M Jenkins and J T Parker 1992 *Appl. Phys. Lett* **611754**-6
[17] L H Frandsen, A V Lavrinenko and P I Borel 2006 *Opt. Express* **14**(20) 9444-9450
[18] V Chheang, T K Lee and GY Oh 2013 *Opt. Express* **21**(18) 20880-87